

Article

Inversion Study on Parameters of Cascade Coexisting Gas-Bearing Reservoirs in Huainan Coal Measures

Baiping Chen ¹, Bo Liu ², Yunfei Du ¹, Guoqi Dong ¹, Chen Wang ¹, Zichang Wang ¹, Ran Wang ¹ and Fan Cui ^{1,*}

¹ College of Geosciences and Surveying Engineering, China University of Mining and Technology-Beijing, Ding No. 11 Xueyuan Road, Haidian District, Beijing 100083, China

² School of Earth Science and Engineering, Hebei University of Engineering, No. 19 Tai Chi Road, Economic and Technological Development Zone, Handan 056083, China

* Correspondence: cuifan_cumtb@126.com

Abstract: The prediction and development of three gases, mainly coalbed methane, shale gas, and tight sandstone gas, in the Huainan coal measures of China, has been the focus of local coal mines. However, due to the overlapping and coexisting characteristics of the three gas reservoirs in Huainan coal measure strata, it is challenging to develop the three gas. The coal mine has been creating a single pool for a long time, resulting in the severe waste of other gas resources in developing the gas-bearing resources in the coal measure strata. The gas-containing reservoir is predicted based on geological, seismic, and logging in Huainan Mining. In addition, determining the excellent area for reference for the development of three gas resources. First, using logging data, mathematical–statistical methods are used to analyze the physical parameters of gas-bearing reservoirs in multi-layered stacked coal seams. Then, based on the theory of prestack seismic inversion, parameters, such as the impedance of P-wave, the ratio of P-wave velocity and S-wave, Lamé constant, Young’s modulus, and Poisson’s ratio and lithological distribution, are obtained for the whole area. The gas-bearing information of the reservoir is received by the statistics and equation of the parameter intersection diagram and is closely related to exploration and development. Finally, the paper synthetically predicts the most favorable area of the gas-bearing reservoir in the study area. The prediction results are compared with the actual results of coalbed methane content in the existing extraction wells, proving that the method is feasible and can provide the basis for the deployment and development of the well location.

Keywords: coalbed methane (CBM); prestack seismic inversion; brittle index; gas-bearing property



Citation: Chen, B.; Liu, B.; Du, Y.; Dong, G.; Wang, C.; Wang, Z.; Wang, R.; Cui, F. Inversion Study on Parameters of Cascade Coexisting Gas-Bearing Reservoirs in Huainan Coal Measures. *Energies* **2022**, *15*, 6208. <https://doi.org/10.3390/en15176208>

Academic Editor: Reza Rezaee

Received: 30 June 2022

Accepted: 18 August 2022

Published: 26 August 2022

Publisher’s Note: MDPI stays neutral with regard to jurisdictional claims in published maps and institutional affiliations.



Copyright: © 2022 by the authors. Licensee MDPI, Basel, Switzerland. This article is an open access article distributed under the terms and conditions of the Creative Commons Attribution (CC BY) license (<https://creativecommons.org/licenses/by/4.0/>).

1. Introduction

Currently, the three gases of coal measures in unconventional natural gas, mainly coalbed methane, tight sandstone gas, and shale gas, have been paid attention to and developed in many countries [1]. China is rich in coal resources, ranking third in the world, and has large gas reservoirs in coal measure strata. At the same time, the demand for natural gas is huge, and the natural gas gap is expected to reach 200 billion cubic meters in 2030 [2]. Many researchers have also done a lot of work on predicting and developing coalbed methane in the Huainan area of China [3,4]. However, the gas-bearing reservoirs of coal measure strata in the Huainan area are characterized by many types and superpositions, leading to the waste of other gas resources in developing coal bed methane [5]. However, the characteristics of superimposed and coexisting gas-bearing reservoirs in Huainan coal measures bring difficulties to build and significant challenges to reservoir prediction in the early stage.

The three gas reservoirs (coalbed methane (CBM), shale gas, tight sandstone gas) in the Huainan coal measures are basically in the Carboniferous–Permian coal measures, with geological characteristics, such as diverse natural gas occurrence, lithology variation, and

overlapping of reservoir and caprock, the coexistence of reservoir fluid pressure system, and significant difference in mechanical properties [6]. Therefore, in the prediction of three different gas reservoirs, not only the lithology, buried depth, thickness, gas-bearing characteristics, and other geological factors should be considered, but also the overall sequence stratigraphic framework characteristics of coal measure strata and the energy and pressure differences among superimposed gas bearing systems should be considered. Therefore, it is necessary to integrate many kinds of information, such as reservoir lithology, reservoir buried depth, reservoir thickness, and gas-bearing characteristics, to predict the type of gas reservoir accurately. Currently, 3D seismic prestack inversion is a common method for oil and gas reservoir prediction, which many researchers have studied. For example, Zhou (2017) used the accurate Zoeppritz equation to realize the inversion of two elastic parameters, Young's modulus and Poisson's ratio, to effectively predict the location of shale gas reservoir [7]. Zhang (2020) proposed they would obtain reservoir parameters of porosity, sand index, and density directly from prestack seismic data through a petrophysical model and prestack amplitude variation with offset (AVO) inversion [8]. The 3D seismic prestack inversion first uses logging data for petrophysical analysis to find the rules and differences of elastic physical parameters in gas-bearing and non-gas-bearing reservoirs. It then establishes the interpretation version, which is reasonably applied to prestack seismic inversion to obtain the reservoir lithology and elastic parameters in the whole area. It then predicts the lithology and fluid information of the reservoir. The intersection result of $\lambda \cdot \rho$ and $\mu \cdot \rho$ can be used to indicate the gas-bearing property of the reservoir. At the same time, the brittleness index represents the brittleness of the reservoir, which is conducive to the generation and fracturing of reservoir fractures [9,10]. For example, Yasin et al. (2021) predict the shale reservoir in the Longgamasi area of China in the Sichuan Basin, China with a brittle template and have achieved successful results [11].

In summary, reservoir parameter inversion has been widely used in reservoir prediction. Currently, the research on reservoir parameters of coal measure formation gas mainly focuses on CBM or single coal seam, and there are few studies on superimposed and coexisting three gas. Given the superposition and co-existence characteristics of the complex three gas reservoirs in Huainan coal measure strata of China, this paper comprehensively studies the systematic reservoir parameters of the three gases. It predicts the favorable gas-bearing areas, which play a positive role in the joint exploitation of the three gases and the well location deployment in the Huainan coal mine.

2. Geologic Setting

The study area is located at Zhangji Coal Mine, 20 km west of Fengtai County, Huainan City, Anhui Province, China (Figure 1). The study area is a fully concealed coal-bearing area, and the buried depth is below 600 m, which is lower than the weathering zone of CBM. The coal measure strata, Carboniferous–Permian in age, are covered with a considerable thickness of loose sediments of younger strata, of Tertiary–Quaternary in age, and overlie the Ordovician strata. In more detail, the coal-bearing strata are Taiyuan of Upper Carboniferous, Shanxi Formation of Permian, Lower Shihezi Formation of Permian, and Upper Shihezi Formation of Permian. The target beds of this study are coal-bearing strata of the Permian Shanxi Formation and Upper and Lower Shihezi Formation, mainly delta deposits. The main coal seams that can be mined are 13-1#, 11-2#, 8#, 6#, and 1# from top to bottom, with an average thickness of 5.7 m, 2.4 m, 3 m, 0.8 m, and 7.2 m, respectively. The coal seam roof is mainly composed of mudstone and sandstone, followed by siltstone and sandstone. The base is mainly composed of mudstone and sandstone and partially consists of fine silt and fine sandstone. Faults developed in the south and north edges of the study area, and the number of fractures in the inner minefield is significant but with a small offset. The storage environments and genesis of the three unconventional natural gas in the study area are shown in Table 1.

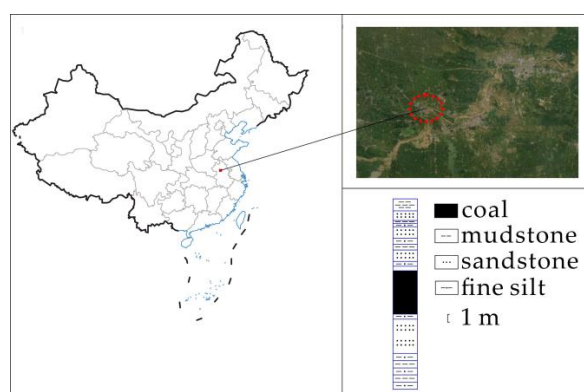


Figure 1. Study area location and lithology histogram.

Table 1. The storage environment and genesis of the three kinds of unconventional natural gas.

	Shale Gas	CBM	Tight Sandstone Gas
Reservoir forming conditions	In situ-generation, in situ-storage, and in situ-preservation	In situ-generation, in situ-storage, and in situ-preservation	Reasonable combination of source, reservoir, and caprock
Definition	It mainly focuses on the natural gas in mud/shale series in adsorption and free state	The natural gas mainly accumulates in coal measure strata in the adsorption state	Under the influence of buoyancy, it focuses on the natural gas at the top of the reservoir
Genetic type	Origin of the thermal evolution of organic matter	Organic matter is formed by thermal evolution and biogenesis	Thermal expansion of organic matter and cracking of crude oil
Occurrence state	20–85% is adsorption; the rest is free and water-soluble	More than 85% of them are adsorbed, and the rest are free and water soluble	The top high points of various traps do not consider the influence factors of adsorption
Reservoir conditions	Characteristics of low porosity and permeability	Dual porosity (matrix and cleat system) Φ : 1–5%; K: 0.5–5.0 md	(1) Low permeability: Φ : 8–20%; K: 0.1–50 md

This study is aimed at gas-bearing reservoirs in coal measure strata. Previous studies believe that AVO has a good prediction effect on gas-bearing reservoirs, so CRP channel gathering seismic data are used to carry out the analysis [12,13]. The frequency band range of this channel is 20–78 Hz, the central frequency is 40 Hz, the offset range is about 0–600 m, and the maximum incidence angle of the target layer is 35 degrees (Figure 2).

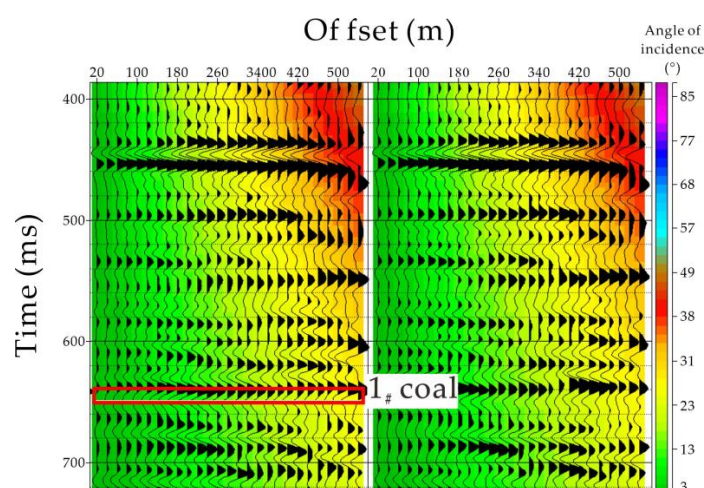


Figure 2. The 3D CRP seismic data profile in the study area.

3. Data and Methods

3.1. Petrophysical Analysis

Coal measure strata are formed in a genetically linked marine–terrestrial or continental sedimentary environment. With this background, CBM, tight sandstone gas, and shale gas reservoirs are layered and co-existed. Their reservoir–cap relationship is complex, and there are conversion changes. There are apparent differences in the types of layer rocks, so a unified petrophysical analysis of the three reservoirs is required [14].

The petrophysical analysis is mainly based on the data of parameter well XX – 1 drilled in 2017 in the study area. This well contains 13-1#, 11-2#, 8#, 6#, and 1# coal layers in the Permian Shanxi Formation. The well was analyzed for reservoir physical parameters by electrical, radioactive, acoustic, and density logging curves, and lithological rules were used to name the formation based on reservoir physical parameters, classifying the lithology into coal rock, tight sandstone gas reservoirs, dry sandstone, shale gas reservoirs, and mudstone. All of the coal rocks contain gas, and the coal rocks can be approximated as coalbed methane reservoirs (Figure 3).

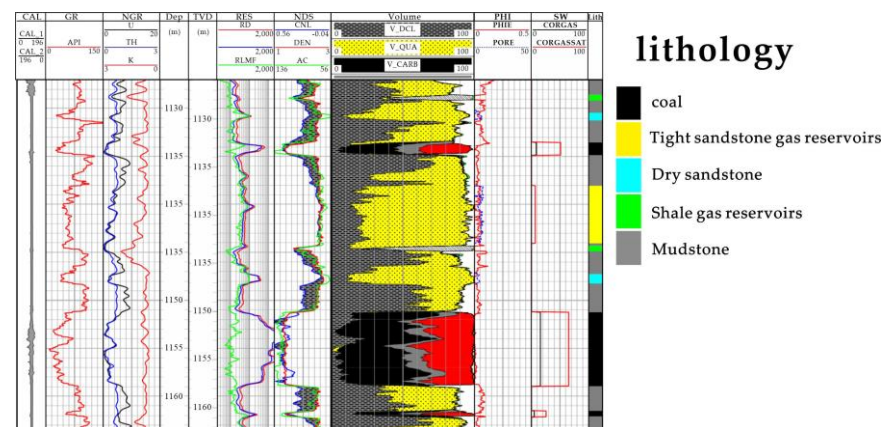


Figure 3. XX – 1 logging interpretation results (Column CAL: borehole diameter curve; Column GR: Gamma curve; Column NGR: energy spectrum curve; Column Dep: depth; Column RES: resistivity curve; Column NDS: Compensated neutron curve, density curve, and acoustic curve; Column Volume: volume of rock physics; Column PHI: porosity curve; Column SW: saturation curve; Column Lith: Lithology).

3.1.1. Relationship between Reservoir Elastic Parameters and Lithology

Reservoir elastic parameters mainly refer to parameters, such as P-wave impedance (Pimp), P-wave velocity (V_p), S-wave velocity (V_s), density, and P-wave to S-wave velocity ratio (V_p/V_s) related to 3D seismic data. These elastic parameters can be directly obtained from the logged data. The ability of adjustable parameters to distinguish lithology is the key to reservoir lithology inversion [15]. In the Carboniferous–Permian coal measure strata, there are many gas-bearing reservoirs, so the intersection of elastic parameters is used to show the distribution law between elasticity and lithology (Figure 4).

3.1.2. Relationship between Reservoir Elastic Parameters and Gas-Bearing Properties

CBM, tight sandstone gas, and shale gas reservoirs have severe overlaps in elastic parameters, and it is challenging to predict gas-bearing reservoirs using conventional flexible parameters. In this study, through the $\lambda \cdot \rho - \mu \cdot \rho$ intersection test and analysis, the recognition effect of gas-bearing reservoirs in the study area is obvious. The distribution is relatively concentrated, which can be used to identify all gas-bearing reservoirs in coal measure strata (Figure 5).

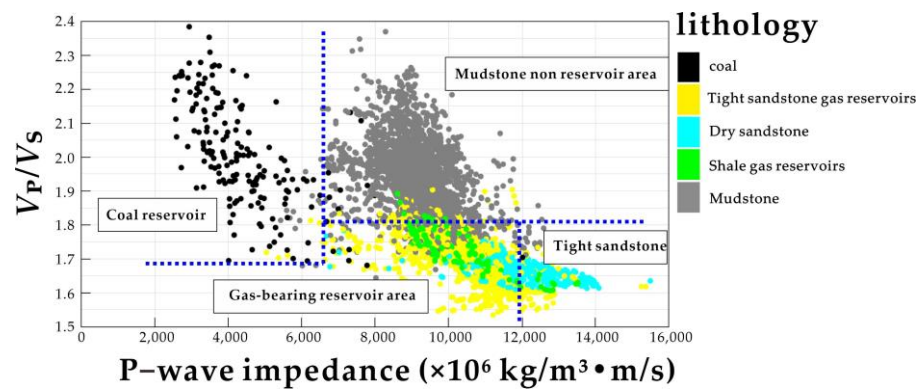


Figure 4. The cross plot of P-wave impedance-P-wave and S-wave velocity ratio after the correction of petrophysics (coal bed is relatively low wave impedance, high P-wave, and S-wave velocity ratio; sandstone gas bed is medium-high wave impedance, low P-wave, and S-wave velocity ratio; dry sandstone bed is relatively high wave impedance, low P-wave, and S-wave velocity ratio; shale gas reservoir is medium-low P-wave impedance, medium-low P-wave velocity ratio).

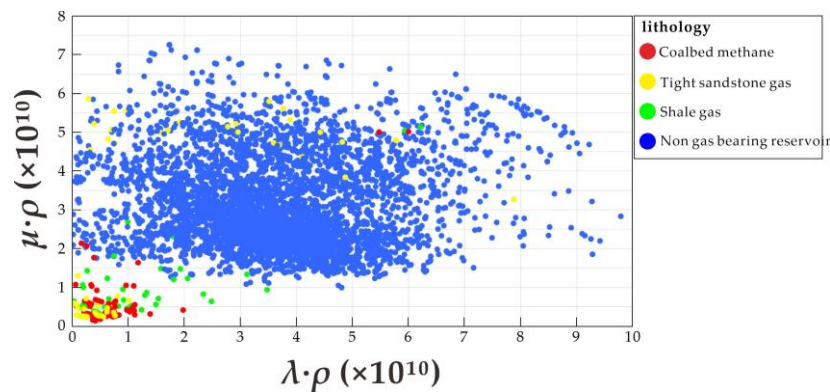


Figure 5. Cross plot of $\lambda \cdot \rho - \mu \cdot \rho$.

3.1.3. The Relationship between Elasticity and Rock Brittleness

The definition of rock brittleness includes two critical parameters: Poisson's ratio and Young's modulus. In the description of the rock mechanics method, the brittleness coefficient is defined by Equations (1)–(3) [16–18]:

$$BI = (YM_{BRIT} + PR_{BRIT})/2, \quad (1)$$

$$YM_{BRIT} = (YMS - YMS_{min})/(YMS_{max} - YMS_{min}), \quad (2)$$

$$PR_{BRIT} = (PR - PR_{max})/(PR_{min} - PR_{max}), \quad (3)$$

In the above Equation: YMS means measured Young's modulus, MPa; PR means measured Poisson's ratio, dimensionless; YM_{BRIT} means normalized Young's modulus, dimensionless; PR_{BRIT} means uniformized Poisson's ratio, dimensionless; BI stands for brittleness index.

XX – 1 Well Poisson's ratio and Young's modulus (static) can be calculated by V_p , V_s , density, and finally, use Equations (1)–(3) to obtain the brittleness index, and give the largest, minimum brittle boundary point feature parameters (Figures 6 and 7). The trend of the most significant friable boundary is high Young's modulus, low Poisson's ratio, and the characteristics of high brittleness and low plasticity. This type of reservoir is conducive to fracturing development; the trend of the minor brittle boundary is low Young's modulus, high Poisson's ratio, and has the characteristics of low brittleness and high plasticity, which is suitable as the cap layer of the reservoir.

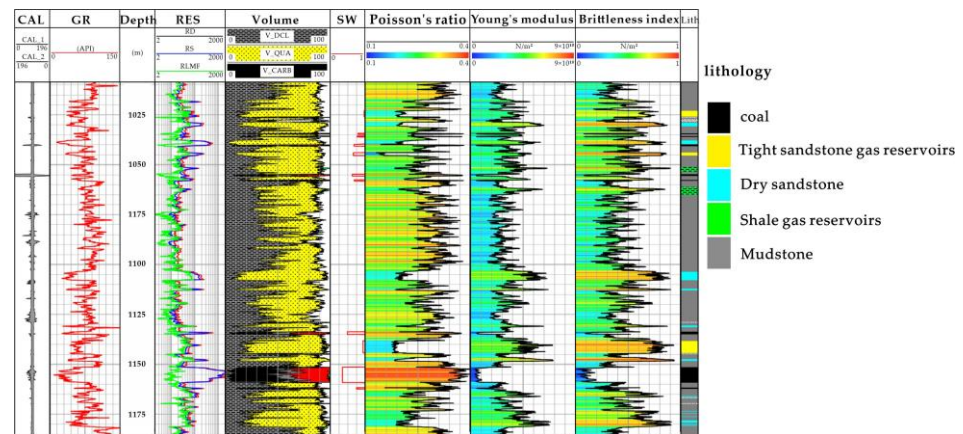


Figure 6. XX – 1 well elasticity and rock brittleness diagram (coal bed gas reservoir shows high Poisson's ratio, low Young's modulus, and low brittleness index; tight sandstone gas reservoir shows low Poisson's ratio, high Young's modulus, and high brittleness index; shale gas reservoir shows middle Poisson's ratio, middle high Young's modulus, and middle high brittleness index).

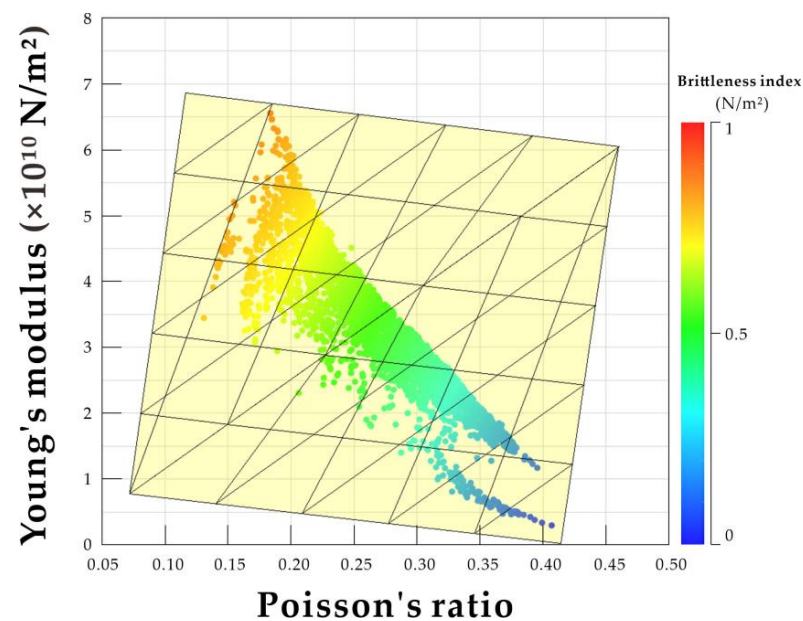


Figure 7. Cross plot of Poisson's ratio and Young's modulus.

3.2. Simultaneous Prestack Inversion

3.2.1. AVO Forward Analysis

AVO response characteristics are affected by the reservoir's longitudinal and transverse wave velocity and density. The CBM content affects the coal reservoir's longitudinal and transverse wave velocity and density. Many researchers have done a lot of research on the forward modeling of conventional gas reservoirs and clearly understand the characteristics of AVO [19–21]. The petrophysical analysis in the study area shows that the elastic parameters of shale gas reservoirs are layered with tight sandstone gas reservoirs, so the AVO types of the two are similar. Considering that the elasticity and physical properties of coal quality are quite different in different regions, this paper carries out AVO forward modeling of the CBM reservoirs in the study area to evaluate the AVO characteristics of the CBM reservoirs. This paper designs 6 different gas saturation models for CBM reservoirs: 0%, 20%, 40%, 60%, 80%, 100% to verify the relationship between CBM content and AVO characteristics. The results show that the intercept attribute has a more obvious response to the enrichment degree of CBM, indicating that the post-stack seismic data will be affected

by the large incident angle seismic data when used in reservoir inversion. Therefore, it is necessary to use prestack seismic data to conduct gas-bearing reservoir prediction research (Figure 8).

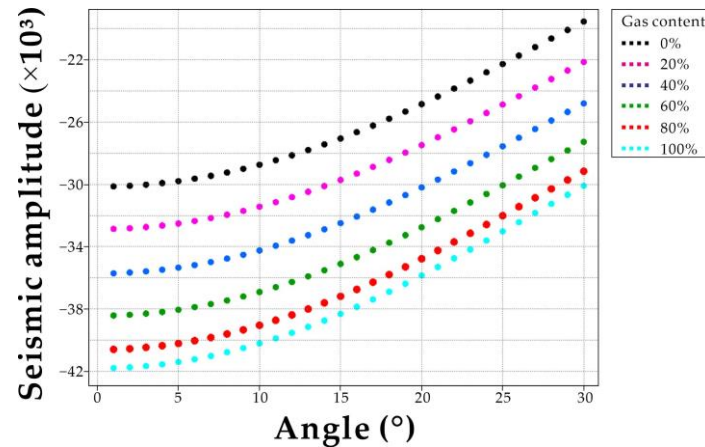


Figure 8. The amplitude of coal roof with different gas content in the forward model varies with the offset (intercept is all negative and decreases with the increase in gas content (absolute value increases), and the degree of decrease becomes smaller. The amplitude increases with the increase in incident angle (offset) (the total value decreases). Gradients are positive and do not change significantly with gas content.

3.2.2. Prestack Gathers Optimization Processing

Reservoir petrophysical research and forward AVO analysis show that the research of gas-bearing reservoirs need to obtain prestack inversion results, such as shear wave impedance, Poisson's ratio, and Lamé constant. The authenticity and accuracy of seismic data directly affect the results of elastic inversion and the accuracy of reservoir prediction. Therefore, this study needs higher requirements for amplitude preservation and fidelity of CRP data. The processing of prestack CRP gathers requires strict amplitude preservation and AVO preservation features. In this study, only noise suppression is performed on seismic gather data. It can be seen that this method reduces noise interference, effectively improves the signal-to-noise ratio, and ensures the quality of the subsequent prestack simultaneous inversion of seismic data (Figure 9).

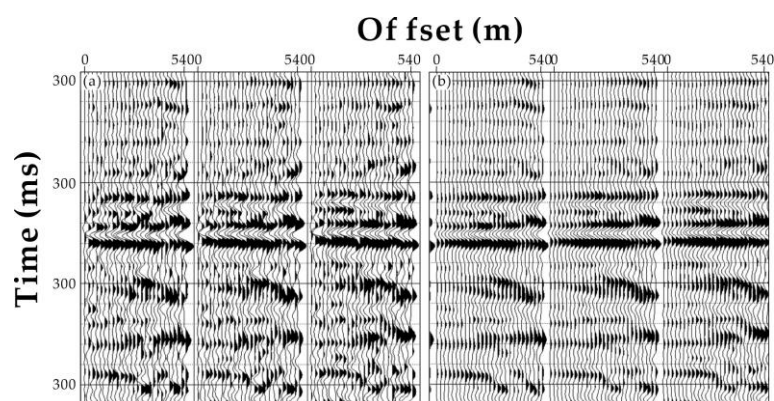


Figure 9. Comparison of 3D seismic tracking data before and after optimization process. (a) is the seismic profile before optimization. (b) is the optimized seismic profile.

Simultaneous prestack inversion requires multiple partially superimposed data volumes with a high signal-to-noise ratio as input. To ensure the stability of the inversion result and a high signal-to-noise ratio, generally, at least 3 to 5 angle gathering superimposed

profiles are required as input data. Due to the low data coverage of the measured channels in this study, the collected data are divided into three-angle parts, superimposed according to the maximum incident angle. Namely, the angle part superimposes 1~12 degrees, 12~24 degrees, and 24~35 degrees (Figure 10).

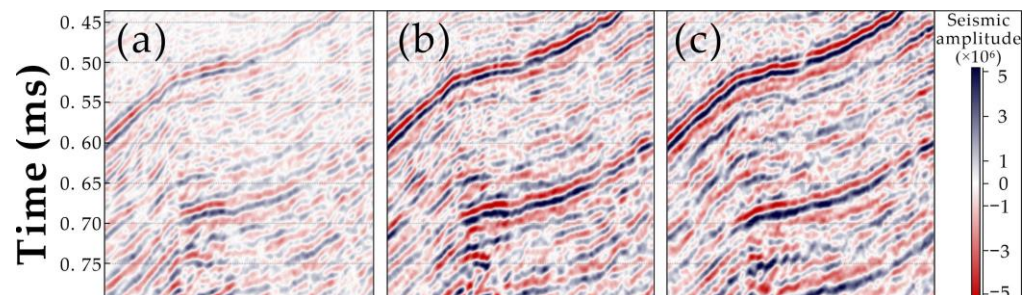


Figure 10. Partial overlay of angle data ((a) Partial overlay of angle 1–12°, (b) Partial overlay of angle 12–24°, (c) Partial overlay of angle 24–35°).

3.2.3. Prestack Inversion

Prestack inversion is also called simultaneous inversion. P-wave velocity and S-wave velocity are calculated together with density [22]. This inversion is performed on the prestack seismic data (incident angle superimposed data or offset superimposed data). Finally, the reservoir parameters, such as compressional wave impedance, density, $\lambda \cdot \rho$, $\mu \cdot \rho$, etc., are obtained. The fluid category is of great significance, and the method is mainly based on the elastic impedance equation (Equations (4)) [23,24].

$$R_{PP}(\theta) = \frac{\Delta\lambda}{\lambda} \left[\frac{1}{4} - \frac{1}{2} \left(\frac{v_s}{v_p} \right)^2 \right] \left(\sec^2\theta \right) + \frac{\Delta\mu}{\mu} \left(\frac{v_s}{v_p} \right)^2 \left(\frac{1}{2} \sec^2\theta - 2\sin^2\theta \right) + \left[\frac{1}{2} - \frac{1}{4} \sec^2\theta \right] \frac{\Delta\rho}{\rho} \quad (4)$$

Among them: V_p is the longitudinal wave velocity, V_s is the transverse wave velocity, and ρ is the density.

The prestack inversion part mainly includes the data needed in angle-stacked seismic data, wavelet, and low-frequency trend model. In the process of inversion, they used a constrained light pulse global optimization method for different incidence angles of multiple seismic data volumes simultaneously inversion. This method objectively uses pre-seismic data information to ensure the reliability of the anti-elastic parameters. The inversion process is shown in Figure 11.

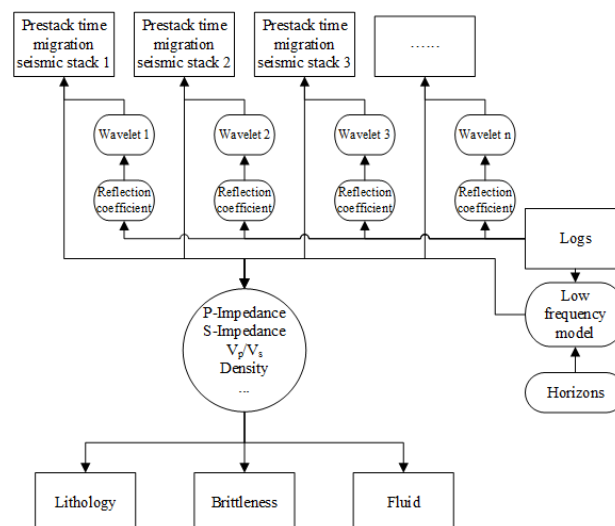


Figure 11. Prestack simultaneous inversion flow.

Obtain P-wave impedance body, P-wave velocity ratio body, density body, $\lambda \cdot \rho$, $\mu \cdot \rho$, Poisson's ratio, and other data bodies (Figure 12). The emphasis of these elastic parameters in geological interpretation is different. The petrophysical analysis shows that the P-wave impedance and P-wave velocity ratios are related to lithology, $\lambda \cdot \rho$ and $\mu \cdot \rho$ are related to gas-bearing properties, and Poisson wave and Young's modulus (static) are related to brittleness index. This is the subsequent geological explanation that provides a basis.

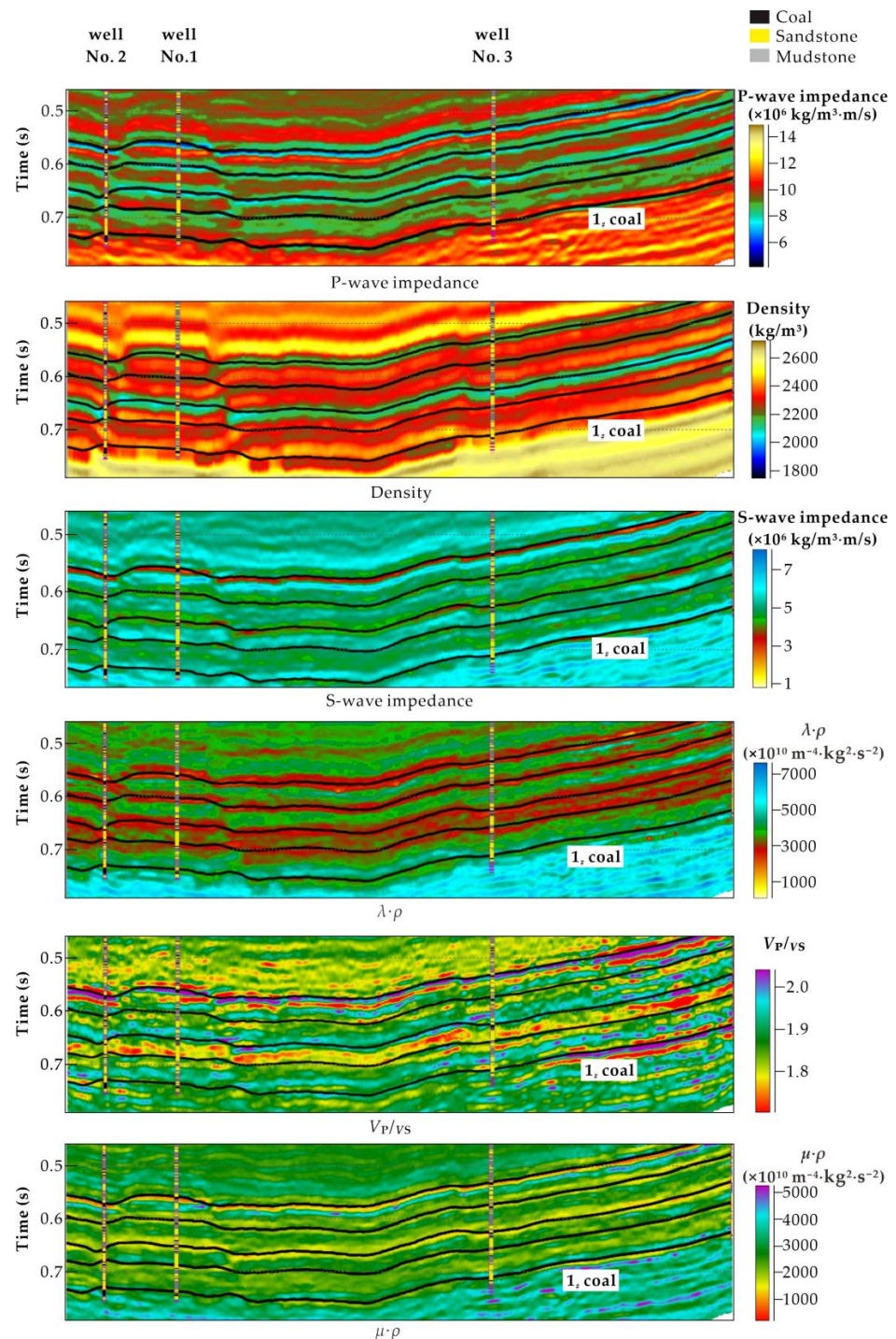


Figure 12. Parameter profiles of P-wave impedance, P-wave velocity ratio, density, $\lambda \cdot \rho$, $\mu \cdot \rho$, and Poisson's ratio.

3.3. Analysis of Brittleness Index

Log brittleness index results show that Poisson's ratio and Young's modulus jointly determine the brittleness index. Based on Equations (1)–(3), the brittleness index is calculated using the inverted Poisson's ratio and Young's modulus (Figure 13). A high value indicates that the formation is brittle and vice versa.

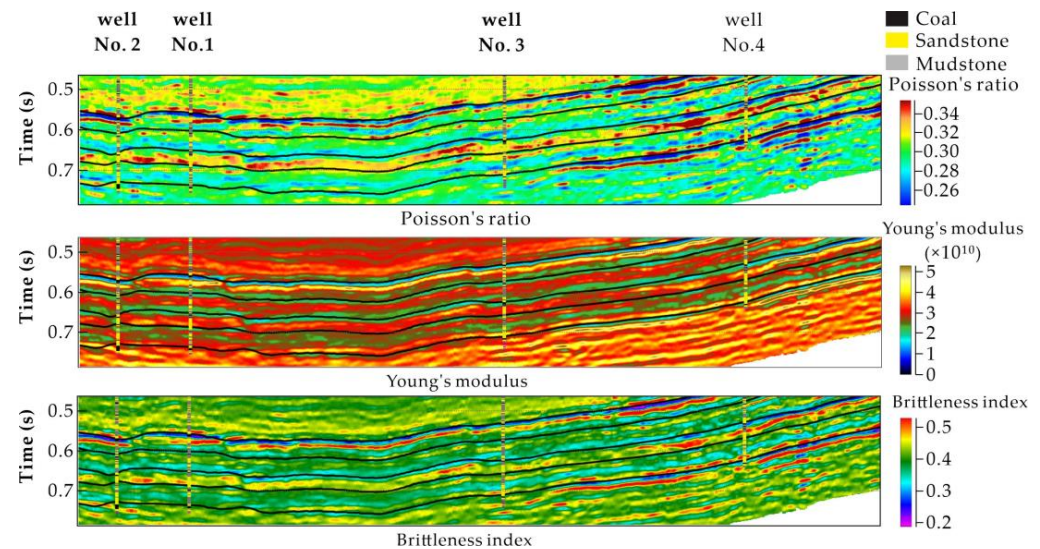


Figure 13. Profiles Poisson's ratio, Young's modulus, Brittleness index inversion.

3.4. Probability Analysis of Lithologic Fluid

The probabilistic analysis process of lithologic fluid is as follows: firstly, the reservoir parameter bodies, such as P-wave impedance, P-wave velocity ratio, density, $\lambda \cdot \rho$, $\mu \cdot \rho$, Poisson's ratio, etc., are obtained by simultaneous prestack inversion, and then based on the results of rock physics analysis, probabilistic analysis of the conversion results in the lithology and fluid spatial distribution [25]. The traditional interpretation process uses the method of elastic parameter cut-off value. This method cannot accurately describe the uncertainty and has large errors. However, the probabilistic volume analysis technology of lithological fluid overcomes these problems. It combines the deterministic petrophysical relationship with statistics, and statistical techniques are used to describe the uncertainty and spatial changes transmitted during the transformation of rock properties [26]. Through lithology statistics and random simulation of the well point data, the response range and quantitative probability distribution function of different lithologies or fluids corresponding to the inversion data volume are established, and the posterior probability of each lithofacies (fluid) is calculated. Finally, the inversion parameters of the reservoir are converted into lithologic bodies and gas-bearing reservoir probabilistic bodies under seismic resolution by two-dimensional table transformation [27]. This paper uses $\lambda \cdot \rho$, $\mu \cdot \rho$ parameters to predict the gas-bearing properties of coal-measure formations and predicts the lithology based on the parameters of P-wave impedance and P-wave velocity ratio. The superimposed study of lithology and gas-bearing properties will be beneficial for storage. The warm-red color in the figure represents the high gas-bearing probability developed in different lithologies. Among them, coal bed methane reservoirs are the main gas-bearing reservoirs of coal-measure strata, followed by tight sandstone gas reservoirs and shale gas reservoirs. There are a few layers that are consistent with the actual logging interpretation (Figure 14).

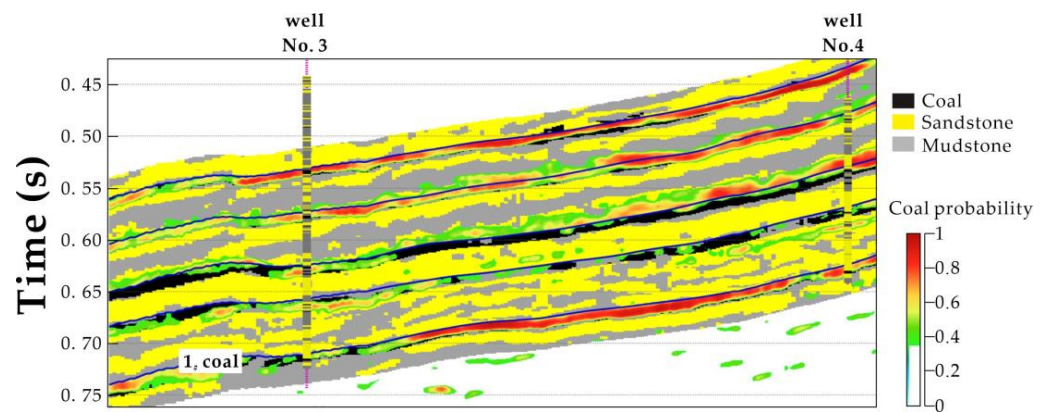


Figure 14. Inversion profile of lithology and reservoir holdup.

4. Results

(1) Reserve rock physical characteristics.

Three gas reservoirs are superimposed and developed in this area. The gas-bearing reservoir parameters interpreted by logging are different. Among them, coal bed methane reservoirs generally contain gas; gas saturation is relatively high, reaching above 50%; and the gas saturation of tight sandstone gas reservoirs and shale gas reservoirs is less than 10% (Figure 3).

After comparative analysis, it can be seen that the junction of P-wave impedance and P-wave to S-wave velocity ratio can show the petrophysical distribution of the reservoir more clearly. From this, it can be seen that the gas-bearing reservoir area seriously overlaps the tight sandstone and mudstone non-reservoir areas. Sandstone areas and mudstone non-reservoir areas can be effectively distinguished (Figure 4)

The gas-bearing reservoirs show the characteristics of $\lambda \cdot \rho$ and $\mu \cdot \rho$ double low (Figure 5).

(2) Gas-bearing distribution of coal measure strata.

Based on the analysis and interpretation of the inversion results of various reservoir parameters, the qualitative and quantitative research system is used to delineate the favorable areas and comprehensively predict the gas-bearing reservoirs. There are five sets of main coal seams in the study area. The study shows that the gas source of the Huainan coal measure strata is mainly coal bed methane. Considering that the coal bed methane has the characteristics of near-source enrichment and accumulation, the buried depth is a very important factor for coal measure strata [28,29]. So, this sweet spot prediction selected 1# coal seam as the object of research and analysis.

As mentioned earlier, the double low characteristics of $\lambda \cdot \rho$ and $\mu \cdot \rho$ can represent gas-bearing reservoirs, and the distribution of gas-bearing reservoirs in space can be explained uniformly by the method of lithological fluid probability analysis. Figure 15 shows the gas-bearing probability plan of CBM in 1# coal (red color in the figure represents high gas-bearing probability). The location of 1# coal seam in the northern part of the study area is relatively high, and the high probability of gas-bearing reservoirs are widely distributed, which is the first choice for CBM mining. In addition, there is a high probability of gas inclusion in the vicinity of well No. 6.

(3) Lithology distribution of coal measures strata.

Based on the lithology prediction, a plan of the thickness of the 1# coal seam was obtained. It can be seen from the map that the thickness of the 1# coal seam in the study area is thicker and well-developed, and the southern part is relatively wide, which is generally beneficial to the exploitation of CBM.

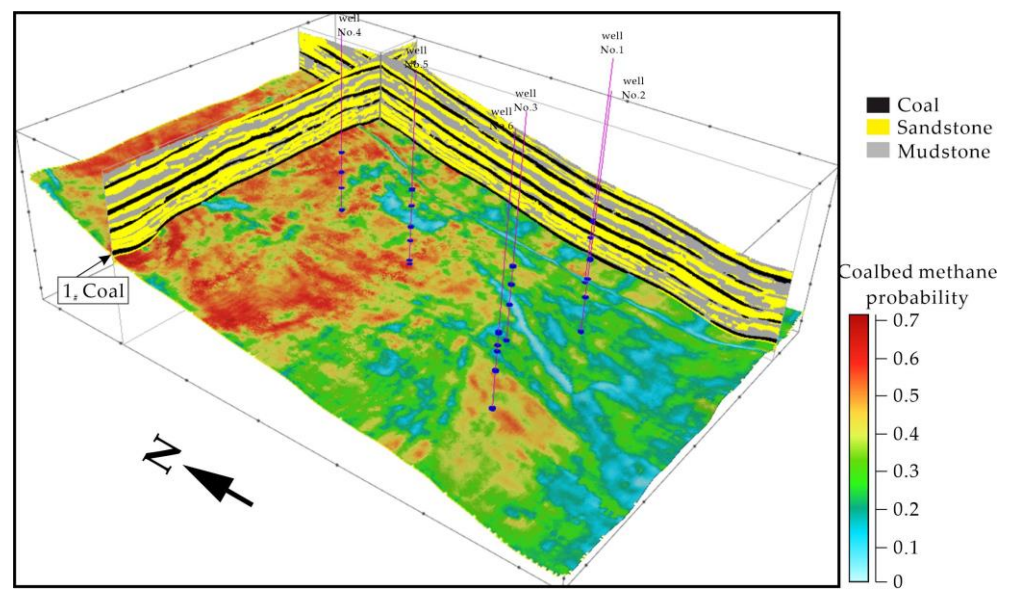


Figure 15. 1# coal seam gas reservoir distribution map.

(4) Analysis of brittleness index of coal measure formation.

The brittleness index plays a vital role in exploiting gas-bearing reservoirs in coal-measure formations, mainly when the utilization level is used for production. It can be seen from the plan of brittleness index extracted from 1# coal seam (Figure 16) that the red area indicates that the coal-measure formation has a high brittleness index, which is mainly located in the northern part of the work area, and cracks are prone to occur during fracturing. In contrast, the brittleness index of the formation in the southern region is low, which is not easy to fracture.

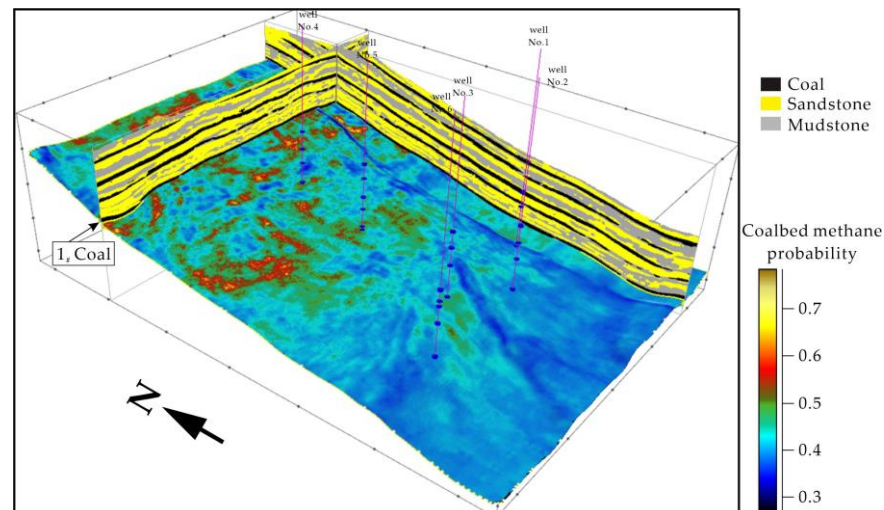


Figure 16. Plan of brittleness index of 1# coal seam.

The prediction of the excellent enrichment area of superimposed and coexisting gas-bearing reservoirs mainly refers to the three reservoir parameters of high gas-bearing capacity, thick coal, and high brittleness index, combined with the characteristics of easy preservation of coal seam gas in areas with deeper structural depths. To delineate the favorable areas of CBM enrichment in the 1# coal seam. The measured results from 72 actual test CBM extraction wells from coal mines were compared with the predicted results. The results show that the CBM reservoirs in relatively high gas content areas are thicker (>0.005 s) and brittle index (>0.5), and the gas content is also high (>0.5). Finally,

the favorable CBM reservoir areas in the study area were delineated, and there were four final delineated areas (Figure 17).

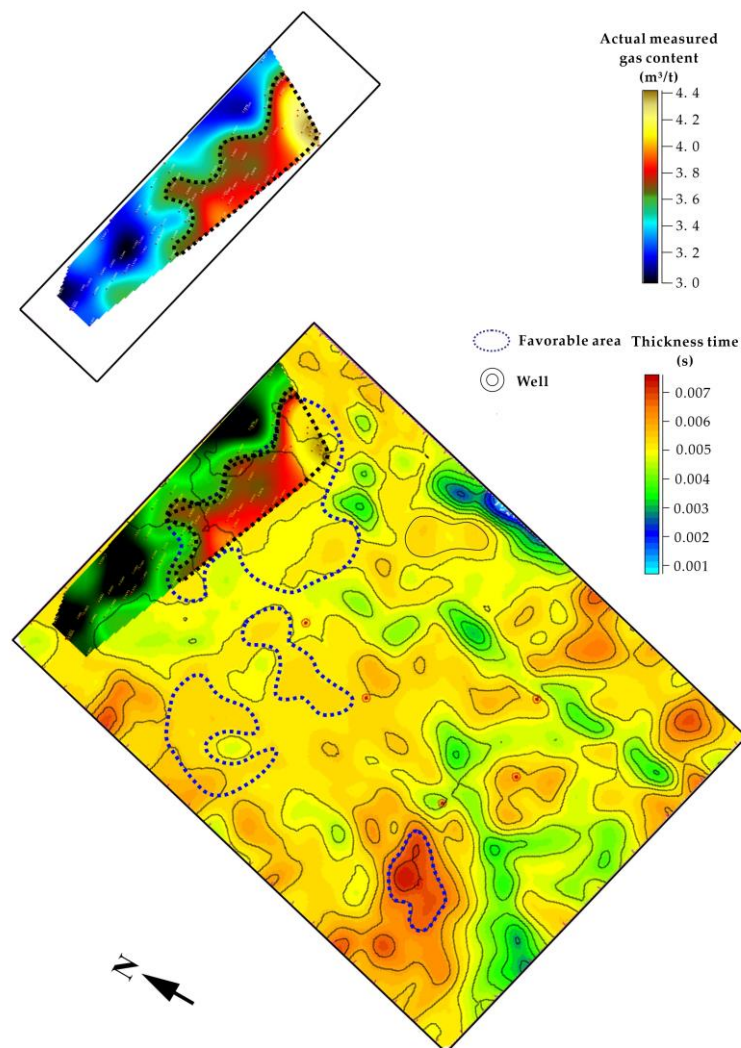


Figure 17. Comparison between actual measurement and prediction results of CBM content.

5. Discussions

The coal seams in the Zhangji coal mine area in Huainan, China are characterized by multiple overlapping layers, which makes the prediction of CBM more difficult. The drilling method has higher detection accuracy for CBM, but the economic cost is higher for large area detection. The geological survey method can realize the detection of large area at lower cost, but the detection accuracy is poor. Considering that the seismic exploration technology has been widely promoted in China's coal field, the 3D seismic prestack inversion method has been successfully used in oil and gas field for reservoir prediction. In this study, the coal seam thickness, tectonics, and petrophysical conditions are considered. Firstly, a petrophysical analysis of the physical properties of CBM reservoirs was conducted, and the correlation between the P-wave impedance of CBM reservoirs and the lithology, fluid factor $\lambda \cdot \rho$, $\mu \cdot \rho$, and brittleness index is summarized. Then, the joint response of CBM fluid factor, coal seam spreading, and brittle distribution information is combined to predict the magnitude of gas-bearing potential of CBM. In order to verify the reliability of the results, statistical analysis of the CBM extraction well data in the existing area of the site was carried out, and the CBM distribution map representing the actual coal content size was drawn and analyzed with the predicted results. The results show that using the criteria of

thickness > 0.005 s, brittleness index > 50%, and gas content > 50% of the CBM reservoir, the possibility of CBM in the study area can be predicted. This method extends the application of the pre-stack seismic simultaneous inversion method in the Huainan coal region of China based on the previous work and improves the accuracy of prediction by combining coal bed distribution, brittleness index, and fluid factor to predict the gas-bearing potential of coalbed methane.

6. Conclusions

Based on the logging data for CBM reservoir petrophysical analysis, the 3D seismic prestack simultaneous inversion method and lithological fluid probability analysis are used to obtain reservoir gas content, brittleness index, reservoir lithology, and thickness information, and to achieve the prediction of the best favorable zone for CBM. The point of this method is that it integrates geological, seismic, and logging data and takes into account various characteristics of the coal thickness, fold structure, gas content, and brittleness index of the CBM reservoir, which improves the accuracy of prediction. From the petrophysical analysis results, the “double low” characteristics of $\lambda \cdot \rho$ and $\mu \cdot \rho$ of CBM reservoir can be derived. By comparing the results with the experimental wells for CBM extraction, it is found that the thick coal seam, high brittleness index, and high gas content can better reflect the best favorable zone for CBM reservoirs. Therefore, the method proposed in this study is important for future CBM and even three gas predictions, reducing the prediction cost and improving the development efficiency.

Author Contributions: B.C.: Conceptualization, Methodology, Writing—Original draft preparation; F.C.: Supervision, Writing—Review and Editing, Validation; B.L.: Resources, Validation; Y.D.: Data curation, Validation; G.D.: Data curation; C.W.: Validation; Z.W.: Validation; R.W.: Visualization. All authors have read and agreed to the published version of the manuscript.

Funding: This work was supported by the open project of State Key Laboratory of Coal Resources and Safe Mining (China University of Mining and Technology-Beijing) (SKLCRSM21KFA04).

Institutional Review Board Statement: Not applicable.

Informed Consent Statement: Not applicable.

Data Availability Statement: Not applicable.

Conflicts of Interest: The authors declare no conflict of interest.

References

1. Xinhua, M. “Extreme Utilization” Development Theory of Unconventional Natural Gas. *Pet. Explor. Dev.* **2021**, *48*, 381–394. [[CrossRef](#)]
2. Jianchao, H.; Zhiwei, W.; Pingkuo, L. Current States of Coalbed Methane and Its Sustainability Perspectives in China. *Int. J. Energy Res.* **2018**, *42*, 3454–3476. [[CrossRef](#)]
3. Tang, B.; Tang, Y.; Wang, C.; Li, Y.; Yu, Y.; Dai, M.; Wang, Z. Rapid co-extraction of coal and coalbed methane techniques: A case study in Zhangji Coal Mine, China. In *Proceedings of the 2019 5th International Conference on Advances in Energy Resources and Environment Engineering (Icaesee 2019)*; Iop Publishing Ltd.: Bristol, UK, 2020; Volume 446, p. 052012.
4. Wei, Q.; Li, X.; Hu, B.; Zhang, X.; Zhang, J.; He, Y.; Zhang, Y.; Zhu, W. Reservoir Characteristics and Coalbed Methane Resource Evaluation of Deep-Buried Coals: A Case Study of the No.13-1 Coal Seam from the Panji Deep Area in Huainan Coalfield, Southern North China. *J. Pet. Sci. Eng.* **2019**, *179*, 867–884. [[CrossRef](#)]
5. Fu, X.; Qin, Y.; Wang, G.G.X.; Rudolph, V. Evaluation of Coal Structure and Permeability with the Aid of Geophysical Logging Technology. *Fuel* **2009**, *88*, 2278–2285. [[CrossRef](#)]
6. Zhang, X.M.; Li, J.W.; Han, B.S.; Dong, M.T. Division and Formation Mechanism of Coalbed Methane Reservoir in Huainan Coalfield, Anhui Province, China. *Chin. Sci. Bull.* **2005**, *50*, 7–17. [[CrossRef](#)]
7. Zhou, L.; Li, J.; Chen, X.; Liu, X.; Chen, L. Prestack Amplitude versus Angle Inversion for Young’s Modulus and Poisson’s Ratio Based on the Exact Zoeppritz Equations. *Geophys. Prospect.* **2017**, *65*, 1462–1476. [[CrossRef](#)]
8. Zhang, F.; Yang, J.; Li, C.; Li, D.; Gao, Y. Direct Inversion for Reservoir Parameters from Prestack Seismic Data. *J. Geophys. Eng.* **2020**, *17*, 993–1004. [[CrossRef](#)]
9. Kang, Y.; Shang, C.; Zhou, H.; Huang, Y.; Zhao, Q.; Deng, Z.; Wang, H.; Ma, Y.Z. Mineralogical Brittleness Index as a Function of Weighting Brittle Minerals—from Laboratory Tests to Case Study. *J. Nat. Gas Sci. Eng.* **2020**, *77*, 103278. [[CrossRef](#)]

10. Russell, B.H.; Hedlin, K.; Hilterman, F.J.; Lines, L.R. Fluid-property Discrimination with AVO: A Biot-Gassmann Perspective. *Geophysics* **2003**, *68*, 29–39. [\[CrossRef\]](#)
11. Yasin, Q.; Sohail, G.M.; Liu, K.-Y.; Du, Q.-Z.; Boateng, C.D. Study on Brittleness Templates for Shale Gas Reservoirs—A Case Study of Longmaxi Shale in Sichuan Basin, Southern China. *Pet. Sci.* **2021**, *18*, 1370–1389. [\[CrossRef\]](#)
12. Gullapalli, S.; Dewangan, P.; Kumar, A.; Dakara, G.; Mishra, C.K. Seismic Evidence of Free Gas Migration through the Gas Hydrate Stability Zone (GHSZ) and Active Methane Seep in Krishna-Godavari Offshore Basin. *Mar. Pet. Geol.* **2019**, *110*, 695–705. [\[CrossRef\]](#)
13. Lu, J.; Wang, Y.; Chen, J.; An, Y. Joint Anisotropic Amplitude Variation with Offset Inversion of PP and PS Seismic Data. *Geophysics* **2018**, *83*, N31–N50. [\[CrossRef\]](#)
14. Tan, P.; Jin, Y.; Han, K.; Zheng, X.; Hou, B.; Gao, J.; Chen, M.; Zhang, Y. Vertical Propagation Behavior of Hydraulic Fractures in Coal Measure Strata Based on True Triaxial Experiment. *J. Pet. Sci. Eng.* **2017**, *158*, 398–407. [\[CrossRef\]](#)
15. Wang, P.; Chen, X.; Wang, B.; Li, J.; Dai, H. An Improved Method for Lithology Identification Based on a Hidden Markov Model and Random Forests. *Geophysics* **2020**, *85*, IM27–IM36. [\[CrossRef\]](#)
16. Gale, J.F.W.; Reed, R.M.; Holder, J. Natural Fractures in the Barnett Shale and Their Importance for Hydraulic Fracture Treatments. *AAPG Bull.* **2007**, *91*, 603–622. [\[CrossRef\]](#)
17. Huo, Z.; Zhang, J.; Li, P.; Tang, X.; Yang, X.; Qiu, Q.; Dong, Z.; Li, Z. An Improved Evaluation Method for the Brittleness Index of Shale and Its Application—A Case Study from the Southern North China Basin. *J. Nat. Gas Sci. Eng.* **2018**, *59*, 47–55. [\[CrossRef\]](#)
18. Rickman, R.; Mullen, M.; Petre, E.; Grieser, B.; Kundert, D. A Practical use of shale petrophysics for stimulation design optimization: All shale plays are not clones of the barnett shale. In Proceedings of the SPE Annual Technical Conference and Exhibition, Denver, CO, USA, 21–24 September 2008; OnePetro: Richardson, TX, USA, 2008; pp. 1–11.
19. Chen, X.-P.; Huo, Q.; Lin, J.; Wang, Y.; Sun, F.; Li, W.; Li, G. Theory of CBM AVO: I. Characteristics of Anomaly and Why It Is So. *Geophysics* **2014**, *79*, D55–D65. [\[CrossRef\]](#)
20. Peng, S.; Chen, H.; Yang, R.; Gao, Y.; Chen, X. Factors Facilitating or Limiting the Use of AVO for Coal-Bed Methane. *Geophysics* **2006**, *71*, C49–C56. [\[CrossRef\]](#)
21. Wang, Y.; Cui, R.; Zhang, S.; Dai, F.; Jia, W. Application of AVO Inversion to the Forecast of Coalbed Methane Area. In *Proceedings of the 2011 Xi'an International Conference on Fine Exploration and Control of Water & Gas in Coal Mines*; Shuning, D., Qun, Z., Li, W., Yongsheng, Q., Yujing, X., Hong, F., Eds.; Elsevier Science: Amsterdam, The Netherlands, 2011; Volume 3, pp. 210–216.
22. Yan, X.; Zhu, Z.; Hu, C.; Gong, W.; Wu, Q. Spark-Based Intelligent Parameter Inversion Method for Prestack Seismic Data. *Neural Comput. Appl.* **2019**, *31*, 4577–4593. [\[CrossRef\]](#)
23. Nolet, G. *Quantitative Seismology, Theory and Methods*; Elsevier: Amsterdam, The Netherlands, 1980.
24. Wu, Q.; Zhu, Z.; Yan, X. Research on the Parameter Inversion Problem of Prestack Seismic Data Based on Improved Differential Evolution Algorithm. *Clust. Comput. J. Netw. Softw. Tools Appl.* **2017**, *20*, 2881–2890. [\[CrossRef\]](#)
25. Yenwongfai, H.D.; Mondol, N.H.; Faleide, J.I.; Lecomte, I. Prestack Simultaneous Inversion to Predict Lithology and Pore Fluid in the Realgrunnen Subgroup of the Goliat Field, Southwestern Barents Sea. *Interpret. J. Subsurf. Charact.* **2017**, *5*, SE75–SE96. [\[CrossRef\]](#)
26. Zhao, L.; Geng, J.; Cheng, J.; Han, D.; Guo, T. Probabilistic Lithofacies Prediction from Prestack Seismic Data in a Heterogeneous Carbonate Reservoir. *Geophysics* **2014**, *79*, M25–M34. [\[CrossRef\]](#)
27. Buland, A.; Kolbjørnsen, O.; Hauge, R.; Skjaeveland, O.; Duffaut, K. Bayesian Lithology and Fluid Prediction from Seismic Prestack Data. *Geophysics* **2008**, *73*, C13–C21. [\[CrossRef\]](#)
28. Wei, Q.; Hu, B.; Li, X.; Feng, S.; Xu, H.; Zheng, K.; Liu, H. Implications of Geological Conditions on Gas Content and Geochemistry of Deep Coalbed Methane Reservoirs from the Panji Deep Area in the Huainan Coalfield, China. *J. Nat. Gas Sci. Eng.* **2021**, *85*, 103712. [\[CrossRef\]](#)
29. Zhang, Z.; Qin, Y.; You, Z.; Yang, Z. Distribution Characteristics of In Situ Stress Field and Vertical Development Unit Division of CBM in Western Guizhou, China. *Nat. Resour. Res.* **2021**, *30*, 3659–3671. [\[CrossRef\]](#)